Appl. Math. Mech. -Engl. Ed., **38**(11), 1579–1600 (2017)
DOI 10.1007/s10483-017-2280-9

Applied Mathematics and Mechanics (English Edition)

Effects of second diffusing component and cross diffusion on primary and secondary thermoconvective instabilities in couple stress liquids*

R. RAVI[1], C. KANCHANA[2], P. G. SIDDHESHWAR[2,†]

1. Department of Humanities and Sciences, National Institute of Technology Goa, Goa 403401, India;
2. Department of Mathematics, Jnana Bharathi Campus, Bangalore University, Bangalore 560056, India

Abstract Linear and weakly nonlinear analyses are made for the Rayleigh-Bénard convection in two-component couple-stress liquids with the Soret effect. Conditions for pitchfork, Hopf, Takens-Bogdanov, and codimension-two bifurcations are presented. The Lorenz model is used to study the inverted bifurcation. Positive values of the Soret coefficient favor a pitchfork bifurcation, whereas negative values favor a Hopf bifurcation. Takens-Bogdanov and codimension-two bifurcations are not as much influenced by the Soret coefficient as pitchfork and Hopf bifurcations. The influence of the Soret coefficient on the inverted bifurcation is similar to the influence on the pitchfork bifurcation. The influence of other parameters on the aforementioned bifurcations is also similar as reported earlier in the literature. Using the Newell-Whitehead-Segel equation, the condition for occurrence of Eckhaus and zigzag secondary instabilities is obtained. The domain of appearance of Eckhaus and zigzag instabilities expands due to the presence of the Soret coefficient for positive values. The Soret coefficient with negative values enhances heat transport, while positive values diminish it in comparison with heat transport for the case without the Soret effect. The dual nature of other parameters in influencing heat and mass transport is shown by considering positive and negative values of the Soret coefficient.

Key words codimension-two, Eckhaus, inverted, Lorenz, Newell-Whitehead-Segel, Nusselt number, Rayleigh-Bénard, secondary instability, Sherwood number, Takens-Bogdanov, zigzag

Chinese Library Classification O351.2
2010 Mathematics Subject Classification 76Rxx

Nomenclature

A, B, C, D, E,	amplitudes;	D_1,	Soret coefficient;
β_{T},	thermal expansion coefficient;	d,	depth;
β_{S},	solutal expansion coefficient;	g,	acceleration due to gravity;
C_{S},	couple stress parameter;	κ,	thermal diffusivity;
D_{S},	Soret parameter;	Le,	Lewis number;
D_{m},	solutal diffusivity;	μ,	dynamic viscosity;

* Received Dec. 7, 2016 / Revised May 22, 2017
† Corresponding author, E-mail: mathdrpgs@gmail.com

μ_1,	couple-stress viscosity;	T,	temperature;
P,	pressure;	t,	time;
Pr,	Prandtl number;	τ,	scaled time;
q,	wave number;	Θ,	non-dimensional temperature;
R_{T},	thermal Rayleigh number;	(u, v, w),	vertical velocity components;
R_{S},	solutal Rayleigh number;	$\boldsymbol{V}(u', v', w')$,	velocity vector;
ρ,	density;	X, Y, Z,	scaled coordinate.
S,	concentration;		

1 Introduction

Relative to the research activity on thermal convection, the work on thermosolutal convection is quite limited. It is now well known that the two mutually opposing diffusing mechanisms give rise to a wide range of interesting phenomena. In such systems with opposing influence on instability, the existence of a net negative density distribution does not ensure stability. Salt fingering (stationary) and diffusive instabilities (overstable) are of importance in these systems. A linear stability analysis of the two-component system was first performed by Nield and Bejan[1].

Most of the literature on double diffusive convection, however, did not consider coupled molecular diffusion, namely, the cross-diffusion effects of Soret and Dufour. These coupled fluxes are due to irreversible thermodynamic effects. If one of the two properties is temperature, the diffusion of solute due to an applied temperature gradient is called the Soret effect or the thermo-diffusion effect, and the diffusion coupled with it is the Dufour effect or diffusion-thermo effect. In liquids, the Dufour effect is negligibly small.

In the presence of chemically inert micron-sized particles, the suspension can be modelled by Stokes' couple stress liquid whose governing equations can be obtained from Eringen's equations for a micropolar continuum. Siddheshwar and Pranesh[2] were the first to study thermoconvective instabilities in such liquids with the single-buoyancy effect. Malashetty et al.[3] extended this study to a system with a second diffusing component and the Soret effect.

Rudraiah and Siddheshwar[4] considered both Soret and Dufour effects on two-component convection of Newtonian liquids saturating a sparsely-packed porous medium. A very comprehensive account of the cross-diffusion coefficient on finite-amplitude instability and heat and mass transport was presented in the paper. There have been other works that consider thermoconvective instability in the couple-stress liquid with the single-buoyancy effect[5–12].

Thermo-diffusion (Soret effect) and diffusion-thermo (Dufour effect) effects on convective instabilities in nanofluids have been theoretically investigated by Kim et al.[13]. They noticed that both the Soret and Dufour effects make nanofluids unstable, and the heat transfer enhancement by the Soret effect in binary nanofluids is more significant than that in normal nanofluids. Siddheshwar et al.[14] made a detailed study of the effect of Soret coefficient on heat transport in twenty nanoliquids. Wang and Tan[15] investigated stability analysis of double-diffusive convection in a viscoelastic fluid with the Soret effect occupying a porous medium using a modified-Maxwell-Darcy model. They showed that the relaxation time also enhances the instability of the system along with the Soret parameter. Altawallbeh et al.[16] analytically studied double-diffusive convection in an anisotropic porous layer heated and salted from below with an internal heat source and Soret effect using both linear and nonlinear stability analyses. They found that increasing the mechanical anisotropy parameter, the Soret parameter, and the internal Rayleigh number enhances heat and mass transfer. The instability of a horizontal layer of a binary nanofluid in a vertical magnetic field was investigated by Gupta et al.[17] using the normal mode analysis and weighted residual method. Complex expressions for the Rayleigh number were simplified by valid approximations for an analytical study, and numerical investigations were made for the alumina-water nanofluid. They showed that the critical wave number

increases when the Chandrasekhar number increases, and it is independent of the solute and nanoparticles. Agarwal and Rana[18] studied the onset of periodic and aperiodic convection in a binary nanofluid saturated rotating porous layer. They obtained the Rayleigh numbers for stationary and oscillatory convections in terms of various non-dimensional parameters. The effect of the physical parameters on the aperiodic convection was analyzed graphically. The thermal instability using the linear stability analysis in a rotating anisotropic porous medium saturated by a nanofluid was analytically studied by Agarwal et al.[19]. The expression of the Rayleigh number for both stationary and oscillatory convections in the case of the bottom-heavy arrangement was obtained. A reversed trend between the stationary and oscillatory modes for the bottom-heavy and top-heavy arrangements was explained in the paper. Ren and Chan[20] studied double-diffusive convection in a vertical cavity with horizontal temperature and concentration gradients using the lattice Boltzmann method. They showed that an increase in the buoyancy ratio from 0.01 to 2 causes a decrease in the average Nusselt and Sherwood numbers. However, a further increase in the buoyancy ratio from 2 causes an increase. In addition, the double-diffusive flow was observed to be unsteady at a small Prandtl number ($Pr = 0.1$) and large Lewis numbers ($Le > 6$). Hu et al.[21] studied transient growth due to non-normality for the Poiseuille-Rayleigh-Bénard flows of binary fluids with the Soret effect. They considered two cases (i) negative separation factors and (ii) positive separation factors. They showed that for negative separation factors, the transient growth is strong, whereas for positive separation factors, it is weak. They used the least-stable mode for computation. Other noteworthy works considering Soret and/or Dufour effects in their problems were those of Ibrahim et al.[22], Nawaz et al.[23], and Al-Odat and Al-Ghamdi[24].

The works on convection in couple-stress liquids cited above are, however, silent about the following subjects:

(i) Takens-Bogdanov bifurcation,

(ii) codimension-two bifurcation,

(iii) inverted bifurcation,

(iv) Eckhaus and zigzag instabilities,

(v) heat and mass transport.

These aforementioned unconsidered aspects of the two-component thermoconvective instability problem in couple-stress liquids with the Soret effect are studied in the paper using the Lorenz and Newell-Whitehead-Segel equations[25].

2 Basic equations

Consider an infinite extent horizontal couple stress liquid layer of thickness d. The upper and lower boundaries are held at a constant temperature T_0 and $T_0 + \Delta T$ ($\Delta T > 0$), respectively. The solutal concentrations are maintained at S_0 and $S_0 + \Delta S$, respectively. The bounding surfaces of the layer are further assumed to be stress-free, isothermal, and isohaline. The Boussinesq approximation is assumed to be valid. The thermal and solutal gradients lead to simultaneous heat and mass transfer. In mixtures, temperature and concentration gradients induce mass flow, called the Soret effect. With the above effect, heat and mass flows can be expressed as follows:

$$\boldsymbol{J}_{\mathrm{h}} = -\kappa \nabla T', \tag{1}$$

$$\boldsymbol{J}_{\mathrm{m}} = -D_{\mathrm{m}} \nabla S' - D_1 \nabla T', \tag{2}$$

where κ and D_{m} are the thermal conductivity and the mass diffusivity of species, respectively. The quantity D_1 is the Soret coefficient that arises due to cross diffusion. Here, T' is the first diffusing component, and S' is the second diffusing component. Equation (2) signifies the cross-diffusion phenomenon wherein there can be a flux of S' due to $\nabla T'$. Similarly, there can be a flux of T' due to $\nabla S'$, but in the present case, this is assumed to be of negligible magnitude.

Using the above expression, the governing equations[2–3] are written as

$$\nabla' \cdot \boldsymbol{V}' = 0, \tag{3}$$

$$\rho_0\Big(\frac{\partial \boldsymbol{V}'}{\partial t'} + (\boldsymbol{V}' \cdot \nabla')\boldsymbol{V}'\Big) = -\nabla P' + \mu\nabla'^2\boldsymbol{V}' - \mu_1\nabla'^4\boldsymbol{V}' + \rho'\boldsymbol{g}, \tag{4}$$

$$\frac{\partial T'}{\partial t'} + (\boldsymbol{V}' \cdot \nabla')T' = \kappa\nabla'^2 T', \tag{5}$$

$$\frac{\partial S'}{\partial t'} + (\boldsymbol{V}' \cdot \nabla')S' = D_{\mathrm{m}}\nabla'^2 S' + D_1\nabla'^2 T', \tag{6}$$

$$\rho' = \rho_0(1 - \beta_{\mathrm{T}}(T' - T_0) + \beta_{\mathrm{S}}(S' - S_0)). \tag{7}$$

The conduction state is characterized by

$$T_{\mathrm{b}} = \Big(1 - \frac{z'}{d}\Big)\Delta T + T_0, \tag{8}$$

$$S_{\mathrm{b}} = \Big(1 - \frac{z'}{d}\Big)\Delta S + S_0. \tag{9}$$

We use the Cartesian system of coordinates whose dimensional coordinates x', y', and z' are scaled by d. The time t' is scaled by $\frac{d^2}{\kappa}$. The velocity vector $\boldsymbol{V}(u', v', w')$, the temperature T', the concentration S', and the pressure P' are non-dimensionalized by the scales κ/d, ΔT, ΔS, and $\rho_0\kappa^2/d^2$. The dimensionless equations for the perturbed quantities of primary and secondary thermosolutal convective instabilities in two-component couple-stress liquids with the Soret effect are

$$\nabla \cdot \boldsymbol{V} = 0, \tag{10}$$

$$\frac{1}{Pr}\Big(\frac{\partial \boldsymbol{V}}{\partial t} + (\boldsymbol{V} \cdot \nabla)\boldsymbol{V}\Big) = -\frac{\nabla P}{Pr} + \nabla^2\boldsymbol{V} - C_{\mathrm{S}}\nabla^4 V + (R_{\mathrm{T}}\theta - R_{\mathrm{S}}S)\hat{\boldsymbol{e}}_z, \tag{11}$$

$$\frac{\partial \theta}{\partial t} + (\boldsymbol{V} \cdot \nabla)\theta = w + \nabla^2\theta, \tag{12}$$

$$\frac{\partial S}{\partial t} + (\boldsymbol{V} \cdot \nabla)S = w + \frac{1}{Le}\nabla^2 S + D_{\mathrm{S}}\frac{R_{\mathrm{T}}}{R_{\mathrm{S}}}\nabla^2\theta, \tag{13}$$

where

$$R_{\mathrm{T}} = \beta_{\mathrm{T}} g\Delta T d^3/(\kappa\nu), \quad R_{\mathrm{S}} = \beta_{\mathrm{S}} g\Delta S d^3/(\kappa\nu), \quad C_{\mathrm{S}} = \mu_1/(\mu d^2),$$

$$Pr = \mu/(\rho_0\kappa), \quad Le = \kappa/D_{\mathrm{m}}, \quad D_{\mathrm{S}} = D_1\beta_{\mathrm{S}}/(\kappa\beta_{\mathrm{T}}),$$

and the Soret coefficient arises due to cross diffusion.

We apply curl two times on the momentum equation (11) and take the z-component of the resulting equation,

$$\Big(\frac{1}{Pr}\frac{\partial}{\partial t} - \nabla^2 + C_{\mathrm{S}}\nabla^4\Big)\nabla^2 w - R_{\mathrm{T}}\nabla_{\mathrm{h}}^2\theta + R_{\mathrm{S}}\nabla_{\mathrm{h}}^2 S = \frac{1}{Pr}\hat{\boldsymbol{e}}_z \cdot (\nabla \times \nabla \times (\boldsymbol{V} \cdot \nabla)\boldsymbol{V}), \tag{14}$$

where

$$\nabla_{\mathrm{h}}^2 = \frac{\partial^2}{\partial x^2} + \frac{\partial^2}{\partial y^2}.$$

From Eqs. (12)–(14), we get

$$\mathcal{L}w = \mathcal{N}, \tag{15}$$

where

$$\mathcal{L} = \Big(\frac{1}{Pr}\frac{\partial}{\partial t} - \nabla^2 + C_{\rm S}\nabla^4\Big)\Big(\frac{\partial}{\partial t} - \nabla^2\Big)\Big(\frac{\partial}{\partial t} - \frac{1}{Le}\nabla^2\Big)\nabla^2 + R_{\rm S}\Big(\frac{\partial}{\partial t} - \nabla^2\Big)\nabla_{\rm h}^2 + R_{\rm T}\Big(D_{\rm S}\nabla^2 - \Big(\frac{\partial}{\partial t} - \frac{1}{Le}\nabla^2\Big)\Big)\nabla_{\rm h}^2, \tag{16}$$

$$\mathcal{N} = \frac{1}{Pr}\Big(\frac{\partial}{\partial t} - \nabla^2\Big)\Big(\frac{\partial}{\partial t} - \frac{1}{Le}\nabla^2\Big)\hat{\boldsymbol{e}}_z \cdot (\nabla \times \nabla \times (\boldsymbol{V}\cdot\nabla)\boldsymbol{V}) + R_{\rm T}\Big(D_{\rm S}\nabla^2 - \Big(\frac{\partial}{\partial t} - \frac{1}{Le}\nabla^2\Big)\Big)\nabla_{\rm h}^2(\boldsymbol{V}\cdot\nabla)\theta + R_{\rm S}\Big(\frac{\partial}{\partial t} - \nabla^2\Big)\nabla_{\rm h}^2(\boldsymbol{V}\cdot\nabla)S. \tag{17}$$

In the case of small scale convective motions, we may neglect the inertial term (see Siddheshwar and Pranesh[2]), and this is assumed in the paper from here on.

We study the primary instabilities in the next section using the linear stability analysis.

3 Linear stability analysis and study of primary instabilities

We consider stress-free, isothermal, isohaline boundary conditions. In terms of w, the conditions translate into the following ones:

$$w = \frac{{\rm d}^2 w}{{\rm d}z^2} = \frac{{\rm d}^4 w}{{\rm d}z^4} = \frac{{\rm d}^6 w}{{\rm d}z^6} = \frac{{\rm d}^8 w}{{\rm d}z^8} = 0 \quad \text{on} \quad z = 0, 1, \quad \forall x, y. \tag{18}$$

Substituting the normal mode solution

$$w = \sin(\pi z){\rm e}^{{\rm i}qx + {\rm i}\omega t} \tag{19}$$

into the linearized version of Eq. (15), viz., $\mathcal{L}w = 0$, we obtain the dispersion relation,

$$\Big(\delta^2\omega\Big(\frac{{\rm i}\omega}{Pr} + \delta^2(1 + C_{\rm S}\delta^2)\Big)({\rm i}\omega + \delta^2)\Big({\rm i}\omega + \frac{1}{Le}\delta^2\Big) + R_{\rm S}q^2({\rm i}\omega + \delta^2) - R_{\rm T}q^2 D_{\rm S}\delta^2 + R_{\rm T}q^2\Big({\rm i}\omega + \frac{1}{Le}\delta^2\Big)\Big)w = 0, \tag{20}$$

where

$$\delta^2 = \pi^2 + q^2.$$

Performing the classical analysis on Eq. (20), we get the expression of the Rayleigh numbers $R_{\rm Tsc}$ and $R_{\rm Toc}$ for the stationary and oscillatory modes of convection and the expression for the frequency ω in the form of

$$R_{\rm Tsc} = \frac{\delta_{\rm sc}^6(\eta_{\rm sc} + r_{\rm Ssc})}{q_{\rm sc}^2(D_{\rm S}Le + 1)}, \quad R_{\rm Toc} = \frac{I_1}{K}, \quad \omega^2 = \frac{-I_3}{I_2}, \tag{21}$$

where

$$I_1 = q_{\rm oc}^2\delta_{\rm oc}^2\Big(-\frac{1}{Pr}\omega^4 + \delta_{\rm oc}^4\Big(r_{\rm Soc} + \eta_{\rm oc}(1 - D_{\rm S}) - \frac{1}{PrLe^2}(D_{\rm S}Le(Le+1)+1)\Big)\omega^2 + \frac{\delta^8}{Le^2}(Le(r_{\rm S} + \eta_{\rm oc}D_{\rm S}) + \eta_{\rm oc}) + \delta_{\rm oc}^8 D_{\rm S} r_{\rm Soc}\Big), \tag{22}$$

$$I_2 = q_{\rm oc}^2\delta_{\rm oc}^4(1 - D_{\rm S} + \eta_{\rm oc}Pr), \tag{23}$$

$$I_3 = \delta_{\rm oc}^8(q_{\rm oc}^2(\eta_{\rm oc}PrD_{\rm S}Le^2 + (\eta_{\rm oc}Pr + 1)(D_{\rm S}Le + 1)) + r_{\rm Soc}PrLe(Le(D_{\rm S} - 1) + 1)), \tag{24}$$

$$\delta_{\rm sc}^2 = \pi^2 + q_{\rm sc}^2, \quad \delta_{\rm oc}^2 = \pi^2 + q_{\rm oc}^2, \quad K = \frac{q_{\rm oc}^4}{Le^2}(Le^2\omega^2 + \delta_{\rm oc}^4(D_{\rm S}Le + 1)^2),$$

$$r_{\rm Ssc} = \frac{q_{\rm sc}^2 R_{\rm S}}{\delta_{\rm sc}^6}, \quad r_{\rm Soc} = \frac{q_{\rm oc}^2 R_{\rm S}}{\delta_{\rm sc}^6}, \quad \eta_{\rm sc} = 1 + C_{\rm S}\delta_{\rm sc}^2, \quad \eta_{\rm oc} = 1 + C_{\rm S}\delta_{\rm oc}^2,$$

and the subscripts sc and oc denote stationary and oscillatory convections, respectively.

The minimum value of R_{Tsc} is obtained at a minimum (critical) wave number q_{scc}, which is given below,

$$\Big(\frac{q_{\mathrm{scc}}}{\pi}\Big)^4 + 2\Big(\frac{1}{3C_{\mathrm{S}}\pi^2} + \frac{1}{3}\Big)\Big(\frac{q_{\mathrm{scc}}}{\pi}\Big)^2 = \frac{1}{3C_{\mathrm{S}}\pi^2} + \frac{1}{3}. \tag{25}$$

Since the equation governing the critical value of wave number for oscillatory convection does not come in an elegant form as that of q_{sc} above, the same is not recorded here. In Sections 4 and 5, a local nonlinear stability analysis is presented using the Lorenz equation and the Newell-Whitehead-Segel equation.

Using these equations, the inverted bifurcation and Eckhaus and zigzag instabilities are studied.

4 Derivation of fifth-order Lorenz equation at threshold of stationary convection and study of inverted (subcritical) bifurcation

Eliminating the pressure P from Eq. (11), assuming two-dimensional motions, and using the following minimal representation of Fourier series for u, w, θ, and S:

$$u = \pi A(t)\sin(q_{\mathrm{sc}}x)\cos(\pi z), \tag{26}$$

$$w = -q_{\mathrm{sc}}A(t)\cos(q_{\mathrm{sc}}x)\sin(\pi z), \tag{27}$$

$$\theta = B(t)\cos(q_{\mathrm{sc}}x)\sin(\pi z) + C(t)\sin(2\pi z), \tag{28}$$

$$S = L(t)\cos(q_{\mathrm{sc}}x)\sin(\pi z) + M(t)\sin(2\pi z) \tag{29}$$

in the resulting equations from Eqs. (10), (11), (12), and (13), we get the fifth-order Lorenz model in the forms of

$$\frac{\mathrm{d}A}{\mathrm{d}t} = \frac{Pr}{\delta_{\mathrm{sc}}^2}(-\delta_{\mathrm{sc}}^4\eta A - q_{\mathrm{sc}}R_{\mathrm{Tsc}}B + q_{\mathrm{sc}}R_{\mathrm{S}}L), \tag{30}$$

$$\frac{\mathrm{d}B}{\mathrm{d}t} = -q_{\mathrm{sc}}A - \delta_{\mathrm{sc}}^2 B - \pi q_{\mathrm{sc}}AC, \tag{31}$$

$$\frac{\mathrm{d}C}{\mathrm{d}t} = -4\pi^2 C + \frac{\pi q_{\mathrm{sc}}}{2}AB, \tag{32}$$

$$\frac{\mathrm{d}L}{\mathrm{d}t} = -q_{\mathrm{sc}}A - \delta_{\mathrm{sc}}^2 D_{\mathrm{S}}\frac{R_{\mathrm{Tsc}}}{R_{\mathrm{S}}}B - \pi q_{\mathrm{sc}}AM, \tag{33}$$

$$\frac{\mathrm{d}M}{\mathrm{d}t} = \frac{\pi q_{\mathrm{sc}}}{2}AL - 4\pi^2 D_{\mathrm{S}}\frac{R_{\mathrm{Tsc}}}{R_{\mathrm{S}}}C - \frac{4\pi^2}{Le}M. \tag{34}$$

We now use the following scaling, keeping in mind the form of the classical Lorenz model which can be obtained as a particular case obtained in the paper,

$$A = \frac{\pi q_{\mathrm{sc}}A'}{\sqrt{2}\delta_{\mathrm{sc}}^2}, \quad B = \frac{\pi r_{\mathrm{T}}B'}{\sqrt{2}}, \quad C = -\pi r_{\mathrm{T}}C', \quad L = \frac{\pi D'}{\sqrt{2}}, \quad M = \pi E'. \tag{35}$$

Using the scaling (35), the Lorenz system of Eqs. (30)–(34) reduces to

$$\dot{A}' = Pr(B' - \eta_{\mathrm{sc}}A' - r_{\mathrm{Ssc}}D'), \tag{36}$$

$$\dot{B}' = r_{\mathrm{T}}A' - B' - A'C', \tag{37}$$

$$\dot{C}' = A'B' - bC', \tag{38}$$

$$\dot{D}' = A' - \frac{D_{\mathrm{S}}}{r_{\mathrm{Ssc}}}B' - \frac{1}{Le}D' + A'E', \tag{39}$$

$$\dot{E}' = b\frac{D_{\mathrm{S}}}{r_{\mathrm{Ssc}}}C' - \frac{b}{Le}E' - A'D', \tag{40}$$

where

$$b = \frac{4\pi^2}{\delta_{\rm sc}^2}, \quad r_{\rm T} = \frac{q_{\rm sc}^2 R_{\rm Tsc}}{\delta_{\rm sc}^6}, \quad t_1 = t\delta_{\rm sc}^2,$$

and the overdot denotes t_1-derivative.

It is a well known fact in the context of the classical Lorenz model that its trajectories remain within the confines of a sphere. The nonlinear terms are responsible for keeping the trajectories confined. Following Siddheshwar and Titus[26], the trapping region of the trajectories of the solution of the Lorenz model in Eqs. (36)–(40) can be obtained in the form of

$$A'^2 + B'^2 + (C' - r_{\rm T} - Pr)^2 + \frac{D'^2}{(\frac{1}{r_{\rm Ssc}Pr})} + \frac{E'^2}{(\frac{1}{r_{\rm Ssc}Pr})} = (\sqrt{2})^2. \tag{41}$$

From the above equation, we note that the trapping region is a four-ellipsoid in a five-dimensional phase-space.

The Lorenz model of Eqs. (36)–(40) is intractable, but in the steady state, it does possess a solution. The steady-state solution of the Lorenz model of Eqs. (36)–(40) is

$$A'^2 = \frac{-M_2 + \sqrt{M_2^2 - 4M_1M_3}}{2M_1}, \tag{42}$$

$$B' = \frac{br_1A'}{b + A'^2}, \tag{43}$$

$$C' = \frac{r_1A'^2}{b + A'^2}, \tag{44}$$

$$D' = LeA'\Big(1 - \frac{bD_{\rm S}r_{\rm T}}{r_{\rm Ssc}(b + A'^2)} + \frac{LeA'^2}{b + A'^2Le^2}\Big(Le - \frac{bD_{\rm S}r_{\rm T}(Le + 1)}{r_{\rm Ssc}(b + A'^2)}\Big)\Big), \tag{45}$$

$$E' = \frac{-LeA'^2}{b + Le^2A'^2}\Big(Le - \frac{bD_{\rm S}r_{\rm T}}{r_{\rm Ssc}(b + A'^2)}(Le + 1)\Big), \tag{46}$$

where

$$M_1 = \eta_{\rm sc}Le^2, \tag{47}$$

$$M_2 = b\Big(\eta_{\rm sc}(Le^2 + 1) - r_{\rm T}Le^2 + r_{\rm S}Le\Big(1 + Le\Big(1 - \frac{D_{\rm S}r_{\rm T}}{r_{\rm Ssc}}\Big) + Le\Big)\Big), \tag{48}$$

$$M_3 = b^2\Big((\eta_{\rm sc} - r_{\rm T}) + r_{\rm Ssc}Le\Big(1 - \frac{D_{\rm S}r_{\rm T}}{r_{\rm Ssc}}\Big)\Big). \tag{49}$$

Equating the discriminant in Eq. (42) to zero, the finite-amplitude Rayleigh number $R_{\rm T}^{\rm f}$ is obtained as a quadratic equation as follows:

$$\frac{b^2q_{\rm scc}^4Le^4}{\delta_{\rm scc}^{12}}(R_{\rm T}^{\rm f})^2 + \frac{2bq_{\rm scc}^2Le^2}{\delta_{\rm scc}^6}(2b\eta_{\rm sc}(1 + D_{\rm S}Le) - Q_1(1 - D_{\rm S}))R_{\rm T}^{\rm f} + (Q_1^2 - 4\eta_{\rm sc}Le^2Q_2) = 0. \tag{50}$$

Solving Eq. (50), we get

$$R_{\rm T}^{\rm f} = \frac{-Q_4 - \sqrt{Q_4^2 - 4Q_3Q_5}}{2Q_3}, \tag{51}$$

where

$$Q_1 = \eta_{\rm sc} b((Le^2+1) + r_{\rm Ssc} Leb(Le^2 - Le + 1)),$$
$$Q_2 = b^2(\eta_{\rm sc} + r_{\rm Ssc} Le),$$
$$Q_3 = b^2 Le^4 (1 - D_{\rm S})^2,$$
$$Q_4 = 4\eta_{\rm sc} b^2 Le^2 (1 + D_{\rm S} Le) - 2Q_1 bLe^2 (1 - D_{\rm S}),$$
$$Q_5 = Q_1^2 - 4\eta_{\rm sc} Le^2 Q_2.$$

Equation (51) will be used to explore the possibility of inverted (subcritical) bifurcation, and the same is discussed in the results and discussion section. In the next section, we derive the Newell-Whitehead-Segel equation with the intention of using it to study two secondary instabilities, namely, Eckhaus and zigzag instabilities.

5 Derivation of nonlinear two-dimensional Newell-Whitehead-Segel equation at threshold of stationary convection and study of secondary instabilities

In this section, we follow Newell and Whitehead to obtain the Newell-Whitehead-Segel equation governing the amplitude of the imposed disturbance. We assume the manifestation of cylindrical rolls with the axis parallel to the y-axis so that the y-derivatives need not be considered in Eq. (15). The z-dependence comes through the trigonometric functions which ensures that the stress-free boundary condition is satisfied. We use the expansion parameter ϵ as

$$\epsilon^2 = \frac{R_{\rm Tsc} - R_{\rm Tscc}}{R_{\rm Tscc}} \tag{52}$$

to obtain the system of equations of several orders in powers of ϵ. However, the variables x, y, z, and t are scaled as follows:

$$X = \epsilon x, \quad Y = \epsilon^{\frac{1}{2}} y, \quad Z = z, \quad \tau = \epsilon^2 t. \tag{53}$$

The inherent symmetry breaking of instability is reflected through the difference of scaling in the two horizontal directions. In view of Eq. (52), the differential operators can be expressed as

$$\frac{\partial}{\partial x} \to \frac{\partial}{\partial x} + \epsilon \frac{\partial}{\partial X}, \quad \frac{\partial}{\partial y} \to \epsilon^{\frac{1}{2}} \frac{\partial}{\partial Y}, \quad \frac{\partial}{\partial z} \to \frac{\partial}{\partial Z}, \quad \frac{\partial}{\partial t} \to \epsilon^2 \frac{\partial}{\partial \tau}. \tag{54}$$

Due to the fact that we are making a local nonlinear stability analysis, $R_{\rm Tsc}$ is assumed to take values close to the threshold value, $R_{\rm Tscc}$, i.e., $\epsilon \ll 1$. The solution to Eqs. (10)–(13) is now assumed as follows:

$$u = \epsilon u_0 + \epsilon^2 u_1 + \epsilon^3 u_2 + \cdots, \tag{55}$$
$$v = \epsilon^{\frac{1}{2}} v_0 + \epsilon v_1 + \epsilon^{\frac{3}{2}} v_2 + \cdots, \tag{56}$$
$$w = \epsilon w_0 + \epsilon^2 w_1 + \epsilon^3 w_2 + \cdots, \tag{57}$$
$$\theta = \epsilon \theta_0 + \epsilon^2 \theta_1 + \epsilon^3 \theta_2 + \cdots, \tag{58}$$
$$S = \epsilon S_0 + \epsilon^2 S_1 + \epsilon^3 S_2 + \cdots. \tag{59}$$

The first approximation is given by the eigenvector of the linearized problem,

$$u_0 = \frac{\mathrm{i}\pi}{q_{\mathrm{scc}}}(A(X,Y,\tau)\mathrm{e}^{\mathrm{i}q_{\mathrm{scc}}x}\cos(\pi Z) - \mathrm{c.c.}), \tag{60}$$

$$v_0 = 0, \tag{61}$$

$$w_0 = A(X,Y,\tau)\mathrm{e}^{\mathrm{i}q_{\mathrm{scc}}x}\sin(\pi Z) + \mathrm{c.c.}, \tag{62}$$

$$\theta_0 = \frac{1}{\delta^2}(A(X,Y,\tau)\mathrm{e}^{\mathrm{i}q_{\mathrm{scc}}x}\sin(\pi Z) + \mathrm{c.c.}), \tag{63}$$

$$S_0 = \frac{Le(1 - D_{\mathrm{S}}\frac{R_{\mathrm{T}}}{R_{\mathrm{S}}})}{\delta^2}(A(X,Y,\tau)\mathrm{e}^{\mathrm{i}q_{\mathrm{scc}}x}\sin(\pi Z) + \mathrm{c.c.}), \tag{64}$$

where c.c. stands for complex conjugate. Using Eqs. (53) and (54), the linear operator $\mathcal{L}$ in Eq. (16) can be written as

$$\mathcal{L} = \mathcal{L}_0 + \epsilon\mathcal{L}_1 + \epsilon^2\mathcal{L}_2 + \cdots, \tag{65}$$

where

$$\mathcal{L}_0 = \Big(\nabla^6(C_{\mathrm{S}}\nabla^2 - 1)\frac{1}{Le} + \Big(R_{\mathrm{T}}\Big(D_{\mathrm{S}} + \frac{1}{Le}\Big) - R_{\mathrm{S}}\Big)\nabla_{\mathrm{h}}^2\Big)\nabla^2, \tag{66}$$

$$\begin{aligned}\mathcal{L}_1 = {}& \Big(2\frac{\partial^2}{\partial x\partial X} + \frac{\partial^2}{\partial Y^2}\Big)\Big(\frac{-4}{Le}\nabla^6 + \frac{5}{Le}C_{\mathrm{S}}\nabla^8 + \Big(R_{\mathrm{T}}\Big(D_{\mathrm{S}} + \frac{1}{Le}\Big) - R_{\mathrm{S}}\Big) \\ & \cdot(\nabla^2 + \nabla_{\mathrm{h}}^2)\Big),\end{aligned} \tag{67}$$

$$\begin{aligned}\mathcal{L}_2 = {}& \frac{\partial}{\partial\tau}\Big(\Big(1 + \frac{1}{Le}\Big)(1 - C_{\mathrm{S}}\nabla^2)\nabla^6 - (R_{\mathrm{T}} - R_{\mathrm{S}})\nabla_{\mathrm{h}}^2 + \frac{1}{LePr}\nabla^6\Big) \\ & + \Big(2\frac{\partial^2}{\partial x\partial X} + \frac{\partial^2}{\partial Y^2}\Big)^2\Big(R_{\mathrm{T}}\Big(D_{\mathrm{S}} + \frac{1}{Le}\Big) - R_{\mathrm{S}} - (6 - 10C_{\mathrm{S}}\nabla^2)\frac{1}{Le}\nabla^4\Big) \\ & + \frac{\partial^2}{\partial X^2}\Big(\frac{-4}{Le}\nabla^6 + \frac{5}{Le}C_{\mathrm{S}}\nabla^8 + \Big(R_{\mathrm{T}}\Big(D_{\mathrm{S}} + \frac{1}{Le}\Big) - R_{\mathrm{S}}\Big)(\nabla^2 + \nabla_{\mathrm{h}}^2)\Big).\end{aligned} \tag{68}$$

Similarly, the nonlinear term $\mathcal{N}$ in Eq. (17) is taken to be

$$\mathcal{N} = \epsilon\mathcal{N}_0 + \epsilon^2\mathcal{N}_1 + \epsilon^3\mathcal{N}_2 + \cdots, \tag{69}$$

where

$$\mathcal{N}_0 = 0, \tag{70}$$

$$\mathcal{N}_1 = \nabla^2\nabla_{\mathrm{h}}^2\Big(R_{\mathrm{T}}\Big(D_{\mathrm{S}} + \frac{1}{Le}\Big)\theta_0 - R_{\mathrm{S}}S_0\Big)\Big(\frac{\partial u_0}{\partial x} + \frac{\partial w_0}{\partial Z}\Big), \tag{71}$$

$$\begin{aligned}\mathcal{N}_2 = {}& \Big(\nabla^2 + \nabla_{\mathrm{h}}^2\Big)\Big(2\frac{\partial^2}{\partial X\partial x} + \frac{\partial^2}{\partial Y^2}\Big)\Big(\frac{\partial u_0}{\partial x} + \frac{\partial w_0}{\partial Z}\Big) \\ & \cdot\Big(R_{\mathrm{T}}\Big(D_{\mathrm{S}} + \frac{1}{Le}\Big)\theta_0 - S_0\Big) + \nabla^2\nabla_{\mathrm{h}}^2R_{\mathrm{T}}\Big(D_{\mathrm{S}} + \frac{1}{Le}\Big) \\ & \cdot\Big(\frac{\partial}{\partial x}(u_1\theta_0 + u_0\theta_1) + \frac{\partial}{\partial Z}(w_1\theta_0 + w_0\theta_1) + \frac{\partial}{\partial X}(u_0\theta_0)\Big) - \nabla^2\nabla_{\mathrm{h}}^2R_{\mathrm{S}} \\ & \cdot\Big(\frac{\partial}{\partial x}(u_0S_1 + u_1S_0)\frac{\partial}{\partial Z}(w_0S_1 + w_1S_0) + \frac{\partial}{\partial X}(w_0S_0)\Big).\end{aligned} \tag{72}$$

Substituting Eqs. (54), (57), (65), and (69) into Eq. (15), we get

$$\mathcal{L}_0w_0 = 0, \tag{73}$$

$$\mathcal{L}_0w_1 = \mathcal{N}_0 - \mathcal{L}_1w_0, \tag{74}$$

$$\mathcal{L}_0w_2 = \mathcal{N}_1 - \mathcal{L}_1w_1 - \mathcal{L}_2w_0. \tag{75}$$

Equation (73) gives us the expression for the critical Rayleigh number for the onset of stationary convection, viz., Eq. (21).

Using Eqs. (62), (67), and (70) in Eq. (74) and solving them, we get $w_1 = 0$. Using the continuity equation (10), we get $u_1 = 0$. The equations for θ_1 and S_1 are given by

$$\Big(\frac{\partial}{\partial t} - \nabla^2\Big)\theta_1 = w_1 - \Big(u_0\frac{\partial\theta_0}{\partial x} + w_0\frac{\partial\theta_0}{\partial z}\Big), \tag{76}$$

$$\Big(\frac{\partial}{\partial t} - \nabla^2\Big)S_1 = w_1 + \frac{R_\mathrm{T}}{R_\mathrm{S}}\nabla^2\theta_1 - \Big(u_0\frac{\partial S_0}{\partial x} + w_0\frac{\partial S_0}{\partial z}\Big). \tag{77}$$

Substituting Eqs. (54), (57), (58), (59), and (65) into Eqs. (76) and (77), taking $u_1 = w_1 = 0$, and solving the resulting equations, we get

$$\theta_1 = -\frac{1}{2\pi\delta_\mathrm{scc}^2}|A|^2\sin(2\pi z), \tag{78}$$

$$S_1 = \frac{Le}{2\pi\delta_\mathrm{scc}^2}\Big(-Le + D_\mathrm{S}\frac{R_\mathrm{T}}{R_\mathrm{S}}(1+Le)\Big)|A|^2\sin(2\pi z). \tag{79}$$

Substituting Eqs. (62), (67), (68), (71), (78), and (79) in Eq. (75) with $w_1 = 0$ and using the Fredholm alternative condition on the resulting equation, we get the Newell-Whitehead-Segel equation in the form of

$$\lambda_0\frac{\partial A}{\partial\tau} - \lambda_1\Big(\frac{\partial}{\partial X} - \frac{\mathrm{i}}{2q_\mathrm{scc}}\frac{\partial^2}{\partial Y^2}\Big)^2 A - \lambda_2 A + \lambda_3|A|^2 A = 0, \tag{80}$$

where

$$\lambda_0 = \frac{\delta_\mathrm{scc}^6}{Le}(Le+1)(1+C_\mathrm{S}\delta_\mathrm{scc}^2) - \delta_\mathrm{scc}^6(r_1 r_\mathrm{T} - r_\mathrm{S}) + \frac{\delta_\mathrm{scc}^6}{PrLe}, \tag{81}$$

$$\lambda_1 = \frac{4\delta_\mathrm{scc}^6}{Le}\Big(r_\mathrm{S}Le + \frac{2q_\mathrm{scc}^2}{\delta_\mathrm{scc}^2}(3+5C_\mathrm{S}\delta_\mathrm{scc}^2) - r_\mathrm{S}r_\mathrm{T}(D_\mathrm{S}Le+1)\Big), \tag{82}$$

$$\lambda_2 = \frac{\delta_\mathrm{scc}^8}{Le}r_1 r_\mathrm{T}(D_\mathrm{S}Le+1), \tag{83}$$

$$\lambda_3 = \frac{\delta_\mathrm{scc}^6 r_\mathrm{T} r_1}{2Le}(D_\mathrm{S}Le+1) + \frac{r_2\delta_\mathrm{scc}^6}{2}\Big(D_\mathrm{S}Le\frac{r_1}{r_2}r_\mathrm{T} - 1\Big), \tag{84}$$

$$r_1 = \frac{R_\mathrm{T}}{R_{\mathrm{T}\mathrm{scc}}}. \tag{85}$$

Since we consider cylindrical rolls with the axis parallel to the y-axis, we neglect the y-derivatives and the time-derivatives. Equation (80) takes the form of

$$\frac{\mathrm{d}^2 A}{\mathrm{d}X^2} + \frac{\lambda_2}{\lambda_1}\Big(1 - \frac{\lambda_3}{\lambda_2}|A|^2\Big)A = 0. \tag{86}$$

Since $\lambda_1 > 0$, the solution to Eq. (80) turns out to be

$$A(X) = A_0\Big(\tanh\Big(\frac{X}{\Lambda_1}\Big) - 1\Big), \tag{87}$$

where

$$A_0 = (\lambda_2/\lambda_3)^{\frac{1}{2}}, \qquad \Lambda_1 = (2\lambda_1/\lambda_2)^{\frac{1}{2}}. \tag{88}$$

In the succeeding section, Eq. (80) will be used to study the secondary instabilities of Eckhaus and zigzag.

5.1 Secondary instabilities

In terms of fast variables x, y, z, and t, Eq. (80) may be written as

$$\lambda_0 \frac{\partial A}{\partial t} - \lambda_1 \Big(\frac{\partial}{\partial x} - \frac{\mathrm{i}}{2q_{\mathrm{scc}}} \frac{\partial^2}{\partial y^2} \Big)^2 A - \epsilon^2 \lambda_2 A + \lambda_3 |A|^2 A = 0. \tag{89}$$

We now consider the phase-winding solution to Eq. (89) in the form of

$$A(x, y, t) = A_1(x, y, t) \mathrm{e}^{\mathrm{i}(\delta q_{\mathrm{sc}})x}. \tag{90}$$

Substituting Eq. (90) into Eq. (89), we get

$$\begin{aligned} \lambda_0 \frac{\partial A_1}{\partial t} = {} & (\epsilon^2 \lambda_2 - \lambda_1 (\delta q_{\mathrm{sc}})^2) A_1 + 2\mathrm{i}\lambda_1 (\delta q_{\mathrm{sc}}) \Big(\frac{\partial}{\partial x} - \frac{\mathrm{i}}{2q_{\mathrm{sc}}} \frac{\partial^2}{\partial y^2} \Big) A_1 \\ & + \lambda_1 \Big(\frac{\partial}{\partial x} - \frac{\mathrm{i}}{2q_{\mathrm{sc}}} \frac{\partial^2}{\partial y^2} \Big)^2 A_1 - \lambda_3 |A_1|^2 A_1 = 0. \end{aligned} \tag{91}$$

The steady-state uniform solution to Eq. (91) is

$$A_1 = ((\epsilon^2 \lambda_2 - \lambda_1 (\delta q_{\mathrm{sc}})^2) \lambda_3^{-1})^{\frac{1}{2}}. \tag{92}$$

To study the secondary instabilities, we impose an infinitesimal perturbation on the uniform steady state solution in the form of

$$A_1 = ((\epsilon^2 \lambda_2 - \lambda_1 (\delta q_{\mathrm{sc}})^2) \lambda_3^{-1})^{\frac{1}{2}} + \widetilde{u}(x, y, t) + \mathrm{i}\widetilde{v}(x, y, t). \tag{93}$$

Substituting Eq. (93) into Eq. (91) and equating real and imaginary parts on either side of the resulting equation, we get

$$\begin{aligned} \lambda_0 \frac{\partial \widetilde{u}}{\partial t} = {} & \Big(-2(\epsilon^2 \lambda_2 - \lambda_1 (\delta q_{\mathrm{sc}}))^2 + \lambda_1 \Big(\frac{\partial^2}{\partial x^2} + \frac{\delta q_{\mathrm{sc}}}{q_{\mathrm{scc}}} \frac{\partial^2}{\partial y^2} - \frac{1}{4q_{\mathrm{scc}}^2} \frac{\partial^4}{\partial y^4} \Big) \Big) \widetilde{u} \\ & - \Big(2\lambda_1 (\delta q_{\mathrm{sc}}) - \frac{\lambda_1}{q_{\mathrm{scc}}} \frac{\partial^2}{\partial y^2} \Big) \frac{\partial \widetilde{v}}{\partial x}, \end{aligned} \tag{94}$$

$$\begin{aligned} \lambda_0 \frac{\partial \widetilde{v}}{\partial t} = {} & \Big(2\lambda_1 (\delta q_{\mathrm{sc}}) - \frac{\lambda_1}{q_{\mathrm{scc}}} \frac{\partial^2}{\partial y^2} \Big) \frac{\partial \widetilde{u}}{\partial x} \\ & + \lambda_1 \Big(\frac{\partial^2}{\partial x^2} + \frac{\delta q_{\mathrm{sc}}}{q_{\mathrm{scc}}} \frac{\partial^2}{\partial y^2} - \frac{1}{4q_{\mathrm{scc}}^2} \frac{\partial^4}{\partial y^4} \Big) \widetilde{v}. \end{aligned} \tag{95}$$

We analyze Eqs. (94) and (95) by using the normal modes in the form of

$$\widetilde{u} = U \mathrm{e}^{St} \cos(q_x x) \cos(q_y y), \quad \widetilde{v} = V \mathrm{e}^{St} \sin(q_x x) \cos(q_y y). \tag{96}$$

Substituting Eq. (96) into Eqs. (94) and (95), we get

$$(\lambda_0 S + 2(\epsilon^2 \lambda_2 - \lambda_1 (\delta q_{\mathrm{sc}})^2) + \chi_1) U + \lambda_1 q_x \chi_2 V = 0, \tag{97}$$

$$\lambda_1 q_x \chi_2 U + (\lambda_0 S + \chi_1) V = 0, \tag{98}$$

where

$$\begin{aligned} \chi_1 &= \lambda_1 (q_x^2 + (q_y^2 (\delta q_{\mathrm{sc}}))/q_{\mathrm{sc}} + q_y^4/(4q_{\mathrm{sc}}^2)), \\ \chi_2 &= 2(\delta q_{\mathrm{sc}}) + q_y^2/q_{\mathrm{sc}}. \end{aligned}$$

For a non-trivial solution to Eqs. (97) and (98), we require

$$\lambda_0^2 S^2 + 2(2\lambda_0(\epsilon^2\lambda_2 - \lambda_1(\delta q_{\rm sc})^2) + \lambda_0\chi_1)S + (2(\epsilon^2\lambda_2 - \lambda_1(\delta q_{\rm sc})^2) + \chi_1)\chi_1 - q_x^2\lambda_1^2\chi_2^2 = 0. \tag{99}$$

We are not interested in a negative root of Eq. (99), since the mode would then be stable. The positive root of Eq. (99) is

$$S = -\frac{1}{\lambda_0^2}((2\lambda_0(\epsilon^2\lambda_2 - \lambda_1(\delta q_{\rm sc})^2) + \lambda_0\chi_1) + (2\lambda_0(\epsilon^2\lambda_2 - \lambda_1(\delta q_{\rm sc})^2)^2 + \lambda_1^2 q_x^2\chi_2^2)^{\frac{1}{2}}). \tag{100}$$

For this positive root, the rolls can become unstable.

5.2 Eckhaus instability

Substituting $q_y = 0$ in Eq. (99), we get

$$\lambda_0^2 S^2 + 2(2\lambda_0(\epsilon^2\lambda_2 - \lambda_1(\delta q_{\rm sc})^2) + \lambda_0\lambda_1 q_x^2)S + \lambda_1 q_x^2(2(\epsilon^2\lambda_2 - 3\lambda_1(\delta k)^2) + q_x^2) = 0. \tag{101}$$

The possibilities regarding the roots of Eq. (101) are as follows:

(i) both roots are negative, or

(ii) one root is positive, and the other is negative.

When both roots of Eq. (101) are negative (Case (i) above), the product of roots is positive. Both the roots being negative refers to a stable situation.

In Case (ii), the product of roots is negative, and this refers to an unstable situation due to the positive root. By the Descartes rule of sign, the following condition ensures the existence of a positive root:

$$q_x^2 \leqslant 2(3\lambda_1(\delta q_{\rm sc})^2 - \epsilon^2\lambda_2). \tag{102}$$

Since $q_x^2 > 0$, we require

$$\frac{\lambda_2}{\lambda_1} \leqslant \frac{3(\delta q_{\rm sc})^2 R_{\rm Tsc}}{R_{\rm Tsc} - R_{\rm Tscc}}, \tag{103}$$

and this condition defines the domain of Eckhaus instability in the $\left(\frac{\lambda_2}{\lambda_1}, \delta q_{\rm sc}\right)$ plane.

5.3 Zigzag instability

Let us now take $q_x = 0$ in Eq. (99) to get

$$\lambda_0^2 S^2 + 2(2\lambda_0(\epsilon^2\lambda_2 - \lambda_1(\delta q_{\rm sc})^2) + \lambda_0\chi_{11})S + (2(\epsilon^2\lambda_2 - \lambda_1(\delta q_{\rm sc})^2) + \chi_{11})\chi_{11} = 0, \tag{104}$$

where

$$\chi_{11} = \lambda_1(q_y^2(\delta q_{\rm sc})/q_{\rm scc} + q_y^4/4q_{\rm scc}^2).$$

Following the procedure of Subsection 5.2, we can obtain the domain of the zigzag instability in the form of

$$\frac{\lambda_2}{\lambda_1} \leqslant \left(\frac{R_{\rm Tsc}}{R_{\rm Tsc} - R_{\rm Tscc}}\right)\left(2(\delta q_{\rm sc})^2 - \frac{(\delta q_{\rm sc})q_y^2}{q}\right). \tag{105}$$

Having thus far studied the possibility of different types of primary and secondary instabilities, we now quantify the heat and mass transport by considering the stationary instability (primary instability).

6 Heat and mass transports at lower boundary

The heat transport is quantified through the thermal Nusselt number Nu which is defined as

$$Nu = 1 + \left(\frac{-\int_0^{\frac{2\pi}{q_{\rm scc}}} (\frac{\partial \theta}{\partial Z}) \mathrm{d}X}{-\int_0^{\frac{2\pi}{q_{\rm scc}}} (\frac{\mathrm{d}\theta_b}{\mathrm{d}Z}) \mathrm{d}X} \right)_{Z=0}, \tag{106}$$

where

$$\theta_{\rm b} = \frac{T_{\rm b} - T_0}{\Delta T}.$$

Substituting Eqs. (8), (52), (58), (63), and (78) into Eq. (106) and completing integration, we get

$$Nu = 1 + \Big(\frac{R_{\rm Tsc} - R_{\rm Tscc}}{R_{\rm Tscc}} \Big) \frac{q_{\rm scc}}{2\pi \delta_{\rm scc}^2} \int_0^{\frac{2\pi}{q_{\rm scc}}} A^2 \mathrm{d}X. \tag{107}$$

Similarly, mass transport is quantified through the Sherwood number Sh which is defined as

$$Sh = \left(1 + \frac{\int_0^{\frac{2\pi}{q_{\rm scc}}} \Big(\frac{1}{Le} \frac{\partial S}{\partial Z} + D_{\rm S} \frac{R_{\rm T}}{R_{\rm S}} \frac{\partial \Theta}{\partial Z} \Big) \mathrm{d}X}{\int_0^{\frac{2\pi}{q_{\rm scc}}} \Big(\frac{1}{Le} \frac{\mathrm{d}S_{\rm b}}{\mathrm{d}Z} + D_{\rm S} \frac{R_{\rm T}}{R_{\rm S}} \frac{\mathrm{d}\theta_{\rm b}}{\mathrm{d}Z} \Big) \mathrm{d}X} \right)_{Z=0}. \tag{108}$$

Substituting Eqs. (8), (9), (52), (58), (59), (63), (64), (78), and (79) into Eq. (108), we get

$$Sh = 1 + \Big(\frac{R_{\rm Tsc} - R_{\rm Tscc}}{R_{\rm Tscc}} \Big) \frac{q_{\rm scc}}{2\pi \delta_{\rm scc}^2} \Big(\frac{r_{\rm T}}{r_{\rm S}} \frac{r_1}{Le} (Le - 1) + Le \Big) \int_0^{\frac{2\pi}{q_{\rm scc}}} A^2 \mathrm{d}X. \tag{109}$$

In computing Nu and Sh, we make use of Eq. (87) in Eqs. (107) and (109). The next section documents the results and discussion extracted from the computation.

7 Results and discussion

Primary and secondary instabilities are discussed in the paper concerning double diffusive convection in a couple stress liquid, in the presence of the cross diffusion effect of Soret. We first discuss the variation of the critical Rayleigh number for the stationary convection $R_{\rm Tscc}$ and the oscillatory convection $R_{\rm Tocc}$ with the couple stress parameter $C_{\rm S}$ for different values of the solutal Rayleigh number $R_{\rm S}$, the Lewis number Le, the Soret parameter $D_{\rm S}$, and the Prandtl number Pr, and those are shown in Tables 1 and 2. In the above parameters, $C_{\rm S}$ represents the suspended particles, $R_{\rm S}$ represents the Rayleigh number corresponding to the second diffusing component, and $D_{\rm S}$ represents the coupled molecular diffusion or cross-diffusion.

From the tables, one may make the inference that in the presence of suspended particles ($C_{\rm S} \neq 0$), the system is stabilized in the cases of both stationary and oscillatory convection.

The effect of $R_{\rm S}$ on the onset of stationary and oscillatory convection is also shown in Tables 1 and 2. From the tables, we may conclude that when the magnitude of $R_{\rm S}$ increases, the critical Rayleigh numbers of stationary and oscillatory modes increase, thereby indicating that the solutal concentration (second diffusing component) has a stabilizing effect on the onset of convection.

The tables show the effect of the Lewis number Le on the onset of convection for fixed values of the other parameters. With an increase in Le, one can see that the critical Rayleigh number increases in the cases of both stationary and oscillatory convection.

Table 1 Critical values of stationary and oscillatory convection for $D_S = -0.1, 0.1$ (here, OSC refers to oscillatory convection)

D_S	Pr	Le	C_S	R_S	q_{scc}	R_{Tscc}	q_{occ}	ω_c^2	R_{Tocc}	Remark
–0.1	5	7	0.04	1 000	2.045	26 787.7	1.8918	55.2135	2 268.72	OSC
0.1						4 727.25	1.341 5	22.490 3	2 840.7	OSC
	4						1.881 7	53.569 7	2 267.8	OSC
–0.1	6	7	0.04	1 000	2.045	26 787.7	1.891 8	55.213 5	2 268.72	OSC
	8						1.898 8	56.364 9	2 269.59	OSC
	4						1.34	22.24	2 839.23	OSC
0.1	6	7	0.04	1 000	2.045	4 727.25	1.35	23.09	2 827.82	OSC
	8						1.36	23.53	2 822.13	OSC
		5				12 072.6	1.779 9	51.128 7	2 461.28	OSC
–0.1	5	6	0.04	1 000	2.045	17 590.8	1.840 5	53.659 1	2 350.47	OSC
		7				26 787.7	1.891 8	55.213 5	2 268.72	OSC
		5				4 024.21	1.296 5	16.926 5	3 014.06	OSC
0.1	5	6	0.04	1 000	2.045	4 397.7	1.321 5	20.300 1	2 913.72	OSC
		7				4 727.25	1.341 5	22.490 3	2 840.7	OSC
			0.02		2.107 3	26 162.7	1.917 7	61.923 8	2 043.71	OSC
–0.1	5	7	0.04	1 000	2.045 1	26 787.7	1.891 8	55.213 5	2 268.72	OSC
			0.08		1.977 3	28 022.8	1.863 5	46.371 5	2 711.24	OSC
			0.02		2.107 3	4 616.94	1.366 3	28.732 5	2 529.7	OSC
0.1	5	7	0.04	1 000	2.045 1	4 727.25	1.341 5	22.490 3	2 840.7	OSC
			0.08		1.977 3	4 945.2	1.296 9	14.274 7	3 471.08	OSC
				800		22 121.1	1.910 1	47.055 2	2 068.54	OSC
–0.1	5	7	0.04	5 000	2.045	120 121	1.682 4	231.17	6 152.91	OSC
				10 000		236 788	1.313 7	501.101	10 910	OSC
				800		3 903.72	1.315 7	15.049 8	2 678.25	OSC
0.1	5	7	0.04	5 000	2.045	21 197.8	1.311 4	182.069	6 566.46	OSC
				10 000		41 786.1	1.042 5	412.148	11 234.8	OSC

Table 2 Critical values of stationary and oscillatory convections for $D_S = -0.3, 0.3$ (here, PES refers to principle of exchange of stabilities being valid)

D_S	Pr	Le	C_S	R_S	q_{scc}	R_{Tscc}	q_{occ}	ω_c^2	R_{Tocc}	Remark
–0.3	5	7	0.04	1 000	2.045	–7 305.74	2.248 1	104.053	1 861.06	OSC
0.3						2 592.36	1	–7.504 35	3 158.74	PES
	4						2.247 7	100.655	1 843.43	OSC
–0.3	5	7	0.04	1 000	2.045	–7 305.7	2.248 1	104.053	1 861.06	OSC
	6						2.248 7	106.46	1 873.33	OSC
	4						1	–15.381 4	3 317.01	PES
0.3	5	7	0.04	1 000	2.045	2 592.36	1	–15.348 2	3 295.74	PES
	6						1	–15.325 2	3 281.57	PES
		5				–12 073	2.154 5	99.511 1	2 033.82	OSC
–0.3	5	6	0.04	1 000	2.045	–8 795.4	2.207 9	102.28	1 933.61	OSC
		7				–7 305.7	2.248 1	104.053	1 861.06	OSC
		5				2 414.53	1	–15.348 2	3 295.74	PES
0.3	5	6	0.04	1 000	2.045	2 512.97	1	–10.675 3	3 215.61	PES
		7				2 592.36	1	–7.504 35	3 158.74	PES
			0.02		2.107	–7 135.3	2.379	113.021	1 644.54	OSC
–0.3	5	7	0.04	1 000	2.045	–7 305.7	2.248 1	104.053	1 861.06	OSC
			0.08		1.977	–7 642.6	2.115 8	93.082	2 282.03	OSC
			0.02		2.107	2 531.87	1	–1.832 52	2 827.41	PES
0.3	5	7	0.04	1 000	2.045	2 592.36	1	–7.504 35	3 158.74	PES
			0.08		1.977	2 711.88	1	–15.166 6	3 813.25	PES
				800		–6 033	2.204	94.622 9	1 705.01	OSC
–0.3	5	7	0.04	5 000	2.045	–32 760	3.175 5	253.915	5 304.65	OSC
				10 000		–64 579	4.023	388.406	9 598.35	OSC
				800		2 140.75	1	–14.014 1	2 972.76	PES
0.3	5	7	0.04	5 000	2.045	11 624.6	1.098 2	117.282	6 857.55	PES
				10 000		22 914.9	1	285.433	11 522	PES

For positive values of D_S, one can observe from the tables that R_{Tscc} increases with the increase in D_S, while for negative D_S, R_{Tscc} decreases with the increase in $|D_S|$. A similar observation on the effect of D_S on R_{Tocc} can be made. In the case of D_S taking negative values, oscillatory convection is shown to be possible. In the case of positive values of D_S, however, the PES is valid provided $D_S \geqslant 0.3$. Overstability is seen only for the case when the sign of D_S is such as to make a stabilizing contribution to the density gradient.

The tables illustrate the fact that the Prandtl number has a destabilizing effect on oscillatory convection and has no effect on stationary convection.

We now discuss about the possibility of pitchfork, Hopf, Takens-Bogdanov, and codimension-two bifurcations (primary instabilities) using the results of linear stability analysis. The schematic of pitchfork and Hopf bifurcations are shown in Fig. 1.

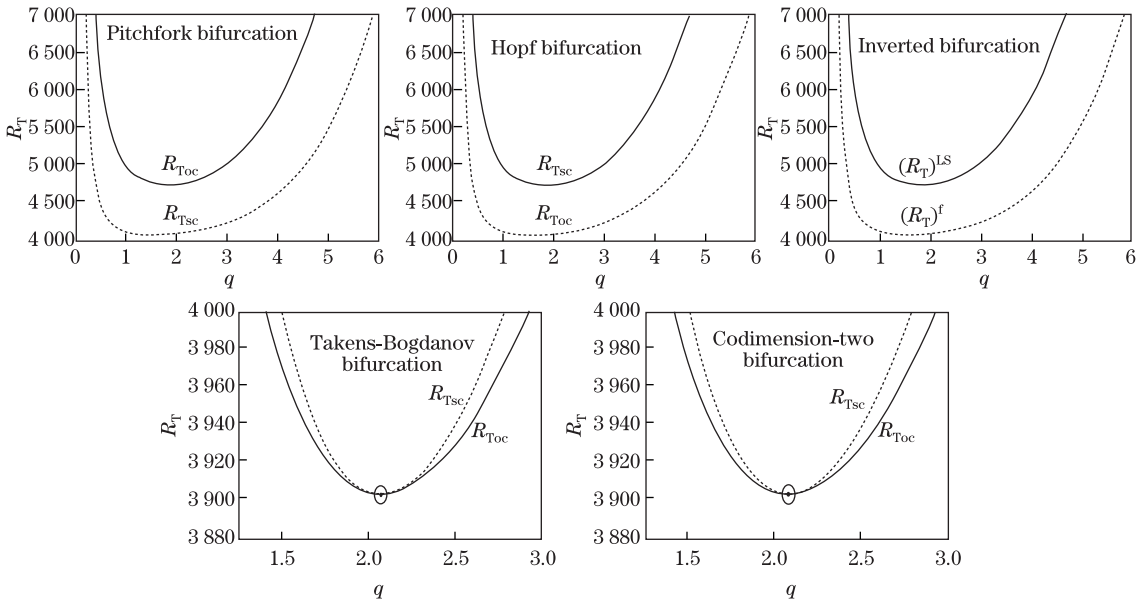

Fig. 1 Schematic of Rayleigh number versus wave number plots for pitchfork, Hopf, inverted, Takens-Bogdanov, and codimension-two bifurcations

Based on the sign of D_S, we may consider the following two cases:

(i) $D_S > 0$ and

(ii) $D_S < 0$.

The pitchfork and Hopf bifurcations are characterized by stationary and oscillatory Rayleigh numbers given by Eq. (21). The finding on the effect of D_S on R_{Tsc} and R_{Toc} is in tune with the results of Malashetty et al.[6] and Hu et al.[21].

From Eq. (84), it is clear that the supercritical pitchfork, subcritical and tricritical bifurcations are, respectively, given by bifurcation $\lambda_3 > 0$, $\lambda_3 < 0$, and $\lambda_3 = 0$ (see Fig. 2). The Takens-Bogdanov bifurcation point is an equilibrium point (here, it is a wave number), at which the neutral curve of oscillatory convection intersects the neutral curve of stationary convection, i.e.,

$$R_{Tocc}(q_{occ}) = R_{Tscc}(q_{scc}), \tag{110}$$

where $q_{oc} = q_{sc}$. If $q_{oc} \neq q_{sc}$, it is called the codimension-two bifurcation point.

Analysing the expression of ω^2 in Eq. (21), we note that when $I_3 = 0$, the frequency on the neutral curve of oscillatory convection approaches zero, i.e.,

$$\omega^2 = 0. \tag{111}$$

Equation (111) is a double zero corresponding to the Takens-Bogdanov bifurcation point at $R_{\mathrm{S}}(q_{\mathrm{oc}})$, where

$$R_{\mathrm{S}}(q_{\mathrm{oc}}) = \frac{\delta_{\mathrm{oc}}^6(Pr(D_{\mathrm{S}}Le(Le+1)+1)(1+C_{\mathrm{S}}\delta_{\mathrm{oc}}^2)+(LeD_{\mathrm{S}}+1))}{q_{\mathrm{oc}}^2 LePr(Le(1-D_{\mathrm{S}})-1)}. \tag{112}$$

The schematic of the Rayleigh number versus the wave number plot corresponding to Takens-Bogdanov and codimension-two bifurcations is shown in Fig. 2.

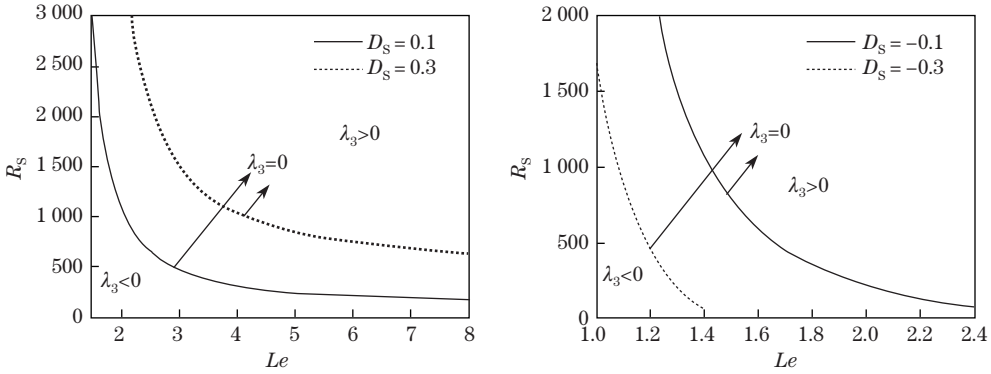

Fig. 2 Plots of R_{S} versus Le obtained from coefficient λ_3 of Newell-Whitehead-Segel equation at onset of stationary convection for $C_{\mathrm{S}} = 0.04$, $Pr = 5$, and $D_{\mathrm{S}} = 0.1, 0.3, -0.1, -0.3$

We now proceed to discuss the results of a nonlinear stability analysis using the Lorenz and Ginzburg-Landau models. The Lorenz model is used to discuss about the possibility of inverted (subcritical) bifurcation. Our findings from the weakly nonlinear stability analysis concur with those of Platten and Chavepeyer[28] and Malashetty et al.[7] that subcritical instability is possible for $D_{\mathrm{S}} < 0$.

Subsection 4.1 discusses the condition under which the secondary instabilities exist. The Ginzburg-Landau equation is used in studying secondary instabilities such as Eckhaus and zigzag.

It is found from our computations that the regions of Eckhaus and zigzag instabilities increase by increasing $|D_{\mathrm{S}}|$ for fixed values of the other parameters (see Fig. 3). However, D_{S} does not significantly alter the region of both Eckhaus and zigzag instabilities.

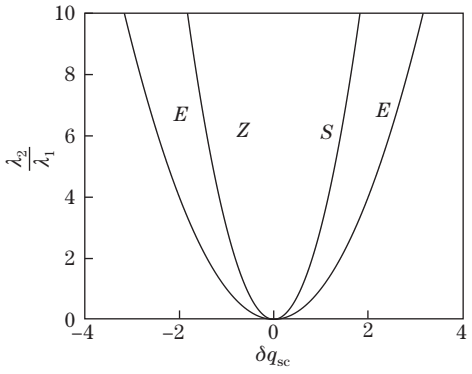

Fig. 3 Plots of secondary instability regions of Eckhaus (E), zigzag (Z) instabilities and stable regions (S) in $(\lambda_2/\lambda_1, \delta q_{\mathrm{sc}})$-plane for $R_{\mathrm{S}} = 1\,000$, $C_{\mathrm{S}} = 0.04$, $Le = 7, D_{\mathrm{S}} = 0.3$, and $Pr = 5$

We evaluate the Nusselt number Nu and the Sherwood number Sh to study heat and mass transport. Figure 4 shows the plots of Nu versus the scaled thermal Rayleigh number r_1 for

different values of the Soret parameter D_S and keeping the other parameters fixed. From the figure, it is clear that for $D_S > 0$, heat transport is diminished, while for $D_S < 0$, heat transport is enhanced compared with the value of Nu of $D_S = 0$.

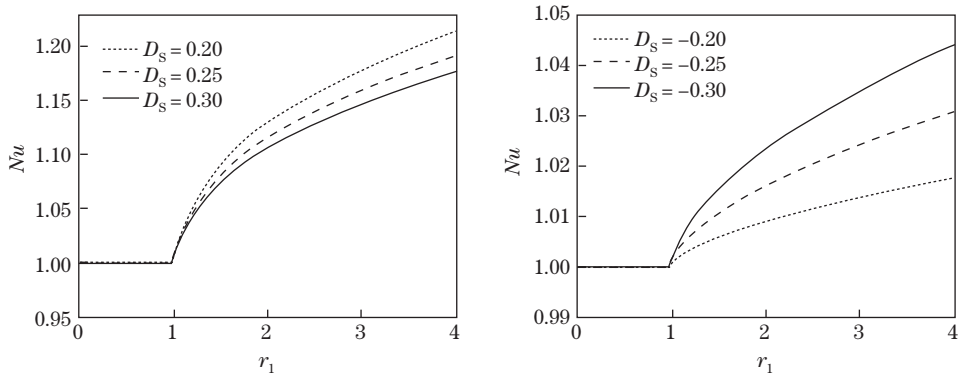

Fig. 4 Plots of Nusselt number Nu versus scaled thermal Rayleigh number r_1 for $C_S = 0.04$, $R_S = 1\,000$, $Le = 7$, and different values of D_S

Figure 5 shows that as we increase Le, Nu increases for $D_S < 0$, while the opposite result is true for $D_S > 0$. Thus, Le enhances heat transport in the case of $D_S < 0$ and diminishes it in the case of $D_S > 0$. A similar effect can be observed in Fig. 6 which is the plot of Nu versus r_1 for different values of C_S.

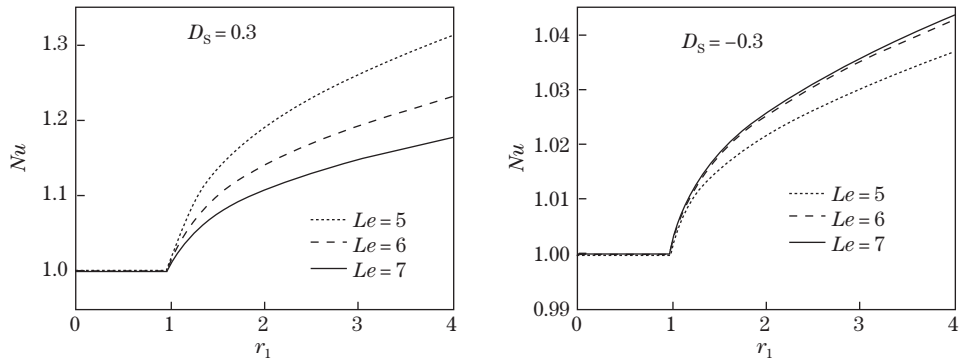

Fig. 5 Plots of Nu versus r_1 for $D_S = 0.3, -0.3$, $C_S = 0.04$, $R_S = 1\,000$, and different values of Le

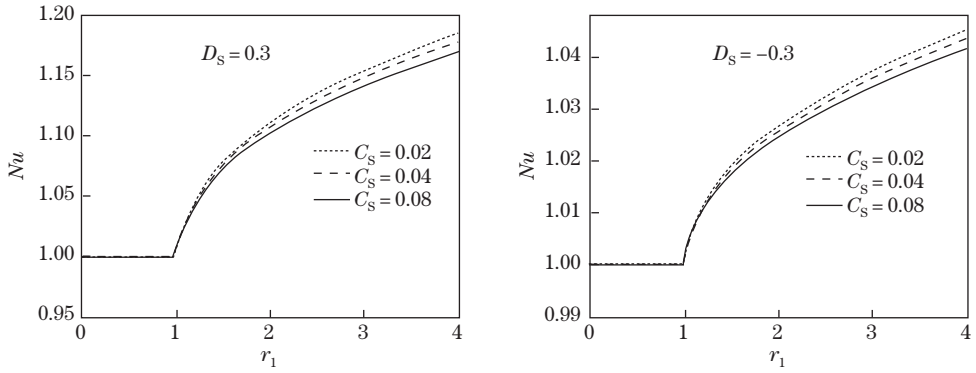

Fig. 6 Plots of Nu versus r_1 for $D_S = 0.3, -0.3$, $R_S = 1\,000$, $Le = 7$, and different values of C_S

Figure 7 throws up an interesting result in the case of $D_S = 0.3$, and the similar result applies for other positive values of D_S. In this case, the second diffusing component fails to alter heat transport of a single component system, and this is essentially due to the cross-diffusion effect signified by the Soret coefficient nullifying the solutal concentration effect on heat transfer. However, in the case of $D_S < 0$, heat transport is significantly altered by the second diffusing component. We also find from the figure that the Nusselt number increases with the increase in R_S.

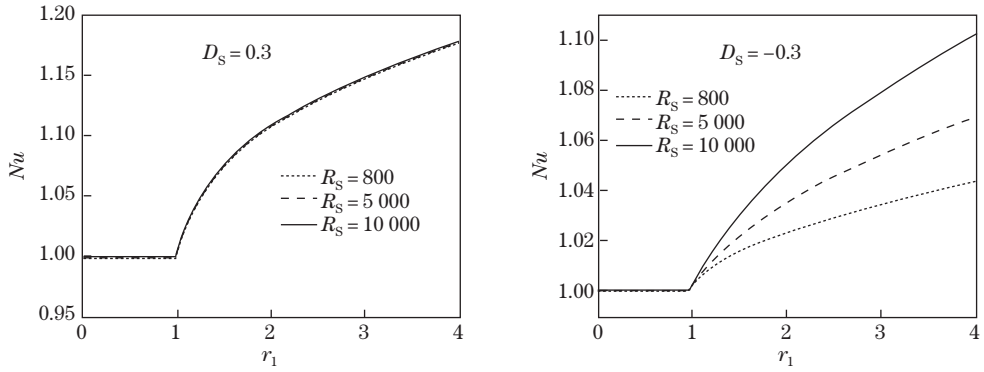

Fig. 7 Plots of Nu versus r_1 for $D_S = 0.3, -0.3$, $C_S = 0.04$, $Le = 7$, and different values of R_S

We next discuss the result on the Sherwood number. From Fig. 8, it is obvious that the solutal transport decreases with an increase in the value of D_S for $D_S > 0$, a result similar to the result on Nu in Fig. 4. Likewise, the results of Figs. 4 and 9 are similar for the case of $D_S < 0$. The effect of Le on Sh for the cases $D_S > 0$ and $D_S < 0$ are qualitatively similar to those of the Nusselt number depicted in Fig. 5 but the only difference is that when Le significantly influences Nu, there is comparatively insignificant influence of Le on Sh. From Eqs. (107) and (109), we may write

$$\frac{Sh - 1}{Nu - 1} = \frac{r_T}{r_S}\frac{r_1}{Le}(Le - 1) + Le < 1. \tag{113}$$

This aspect can be explicitly seen by comparing the corresponding plots of Nu and Sh in Figs. 4–11.

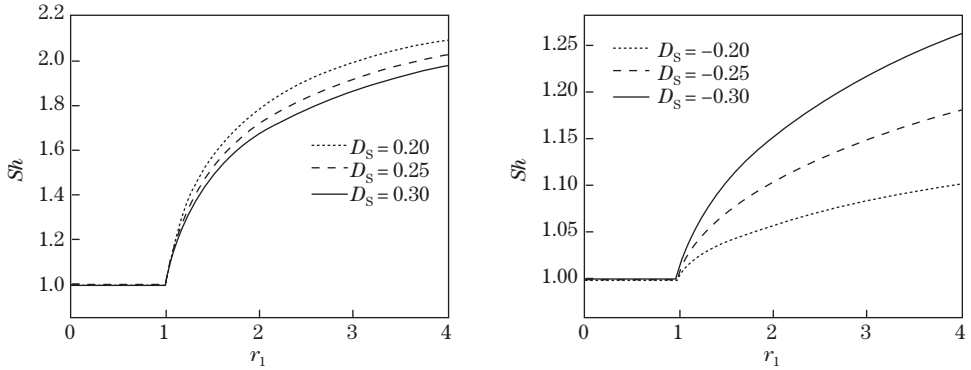

Fig. 8 Plots of Sherwood number Sh versus r_1 for $C_S = 0.04$, $R_S = 1\,000$, $Le = 7$, and different values of D_S

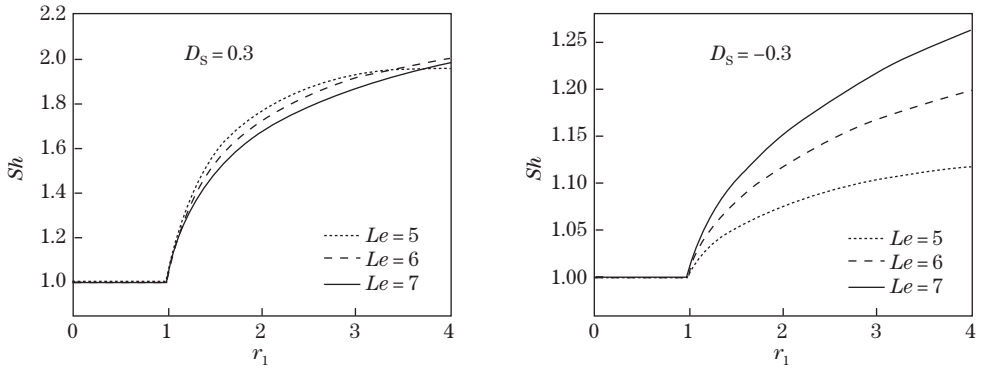

Fig. 9 Plots of Sh versus r_1 for $D_S = 0.3, -0.3$, $C_S = 0.04$, $R_S = 1\,000$, and different values of Le

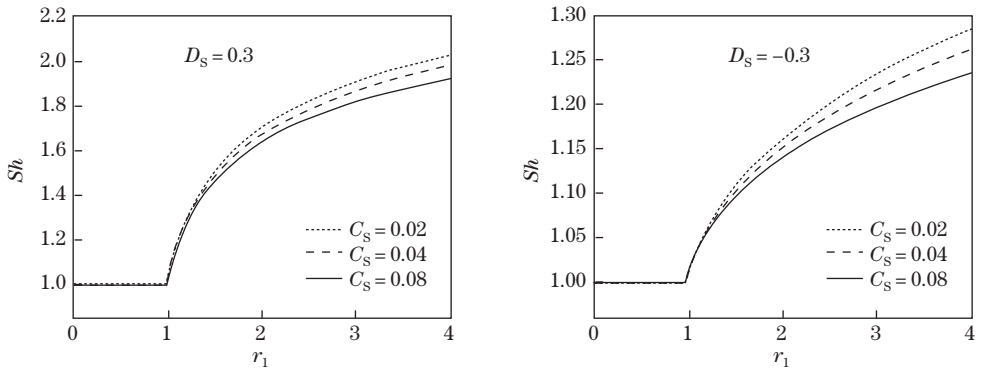

Fig. 10 Plots of Sh versus r_1 for $D_S = 0.3, -0.3$, $R_S = 1\,000$, $Le = 7$, and different values of C_S

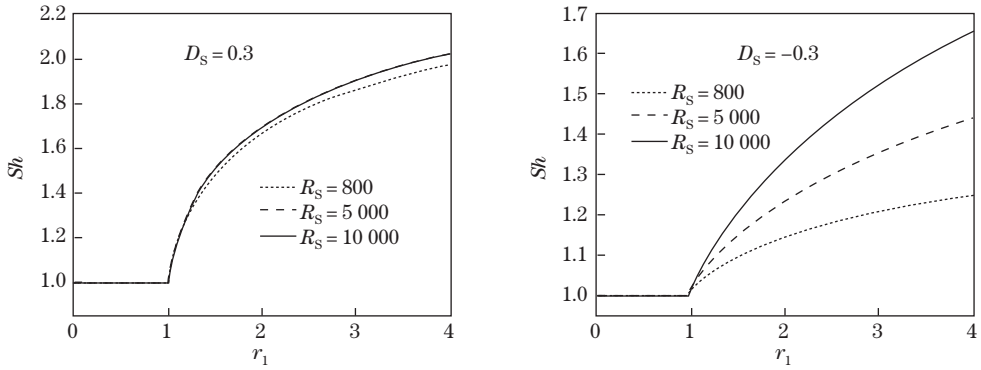

Fig. 11 Plots of Sh versus r_1 for $D_S = 0.3, -0.3$, $C_S = 0.04$, $Le = 7$, and different values of R_S

An important related paper to the current one is the excellent paper by Hu et al.[21] who not only iterated that Poiseuille-Bénard flows are subcritically unstable for negative separation factors but most importantly established that, for very small negative or large positive separation factors and large Rayleigh numbers, the maximum transient growth rate gets enlarged. In the absence of a Poiseuille flow in their Bénard configuration, the results qualitatively match with that of Hu et al.[21,27]. To compare the current paper with the paper of Hu et al.[21], we note the following one-to-one correspondence between the papers:

(i) The separation ratio ψ of Hu et al.[21] is $-\frac{R_S}{R_T}$ of our paper and their Lewis number Le is reciprocal of our Le.

8 Conclusions

(i) The second diffusing component stabilizes the system due to the fact that the solutal concentration increases the density. The Soret effect characterized by D_{S} makes a stabilizing or destabilizing contribution to the density gradient depending on the sign of D_{S}. Overstability is seen only for the case when the sign of D_{S} is such as to make a stabilizing contribution to the density gradient.

(ii) The suspended particles increase the viscosity of the fluid and thereby stabilize the system. The presence of suspended particles is characterized by C_{S}.

(iii) In addition to the pitchfork and Hopf bifurcations, Takens-Bogdanov and codimension-two bifurcations are also possible in the system.

(iv) The inverted (subcritical) bifurcation is possible only for $D_{\mathrm{S}} < 0$.

(v) D_{S} does not alter the regions of the Eckhaus and zigzag instabilities.

(vi) $\frac{\mathrm{d}Nu}{\mathrm{d}D_{\mathrm{S}}} < 0$, $\frac{\mathrm{d}Sh}{\mathrm{d}D_{\mathrm{S}}} < 0$ for $D_{\mathrm{S}} > 0$, and $\frac{\mathrm{d}Nu}{\mathrm{d}|D_{\mathrm{S}}|} > 0$, $\frac{\mathrm{d}Sh}{\mathrm{d}|D_{\mathrm{S}}|} > 0$ for $D_{\mathrm{S}} < 0$.

(vii) Variations of R_{Tsc}, R_{Toc}, Nu, and Sh with Le, C_{S}, and R_{S} for positive and negative values of D_{S} are tabulated in Table 3.

Table 3 Variations of R_{Tsc}, R_{Toc}, Nu, and Sh

R_{Tsc}		R_{Toc}		Nu		Sh	
$D_{\mathrm{S}} > 0$	$D_{\mathrm{S}} < 0$	$D_{\mathrm{S}} > 0$	$D_{\mathrm{S}} < 0$	$D_{\mathrm{S}} > 0$	$D_{\mathrm{S}} < 0$	$D_{\mathrm{S}} > 0$	$D_{\mathrm{S}} < 0$
$\frac{\mathrm{d}R_{\mathrm{Tsc}}}{\mathrm{d}Le}<0$	$\frac{\mathrm{d}R_{\mathrm{Tsc}}}{\mathrm{d}Le}<0$	$\frac{\mathrm{d}R_{\mathrm{Toc}}}{\mathrm{d}Le}>0$	$\frac{\mathrm{d}R_{\mathrm{Toc}}}{\mathrm{d}Le}>0$	$\frac{\mathrm{d}Nu}{\mathrm{d}Le}<0$	$\frac{\mathrm{d}Nu}{\mathrm{d}Le}>0$	$\frac{\mathrm{d}Sh}{\mathrm{d}Le}<0$	$\frac{\mathrm{d}Sh}{\mathrm{d}Le}>0$
$\frac{\mathrm{d}R_{\mathrm{Tsc}}}{\mathrm{d}C_{\mathrm{S}}}>0$	$\frac{\mathrm{d}R_{\mathrm{Tsc}}}{\mathrm{d}C_{\mathrm{S}}}>0$	$\frac{\mathrm{d}R_{\mathrm{Toc}}}{\mathrm{d}C_{\mathrm{S}}}>0$	$\frac{\mathrm{d}R_{\mathrm{Toc}}}{\mathrm{d}C_{\mathrm{S}}}>0$	$\frac{\mathrm{d}Nu}{\mathrm{d}C_{\mathrm{S}}}<0$	$\frac{\mathrm{d}Nu}{\mathrm{d}C_{\mathrm{S}}}<0$	$\frac{\mathrm{d}Nu}{\mathrm{d}C_{\mathrm{S}}}<0$	$\frac{\mathrm{d}Nu}{\mathrm{d}C_{\mathrm{S}}}<0$
$\frac{\mathrm{d}R_{\mathrm{Tsc}}}{\mathrm{d}R_{\mathrm{S}}}>0$	$\frac{\mathrm{d}R_{\mathrm{Tsc}}}{\mathrm{d}R_{\mathrm{S}}}>0$	$\frac{\mathrm{d}R_{\mathrm{Toc}}}{\mathrm{d}R_{\mathrm{S}}}>0$	$\frac{\mathrm{d}R_{\mathrm{Toc}}}{\mathrm{d}R_{\mathrm{S}}}>0$	$\frac{\mathrm{d}Nu}{\mathrm{d}R_{\mathrm{S}}}=0$	$\frac{\mathrm{d}Nu}{\mathrm{d}R_{\mathrm{S}}}>0$	$\frac{\mathrm{d}Nu}{\mathrm{d}R_{\mathrm{S}}}=0$	$\frac{\mathrm{d}Nu}{\mathrm{d}R_{\mathrm{S}}}>0$

Acknowledgements The second author (C. KANCHANA) is grateful to the University Grants Commission (UGC), New Delhi, India for supporting her research work with a Rajiv Gandhi National Fellowship. The authors are grateful to the two reviewers for their educative comments that helped us refine the paper to the present form.

References

[1] Nield, D. A. and Bejan, A. *Convection in Porous Media*, Springer, Singapore (1999)

[2] Siddheshwar, P. G. and Pranesh, S. An analytical study of linear and non-linear convection in Boussinesq-Stokes suspensions. *International Journal of Non-Linear Mechanics*, **39**(1), 165–172 (2004)

[3] Malashetty, M. S., Gaikwad, S. N., and Swamy, M. An analytical study of linear and non-linear double diffusive convection with Soret effect in couple stress liquids. *International Journal of Thermal Science*, **45**, 897–907 (2006)

[4] Rudraiah, N. and Siddheshwar, P. G. A weakly non-linear stability analysis of double diffusive convection with cross diffusion in a fluid-saturated porous medium. *Heat and Mass Transfer* (*Springer*), **33**, 287–293 (1998)

[5] Sharma, R. C. and Thakur, K. D. On couple stress fluid heated from below in porous medium in hydrodynamics. *Czechoslovvak Journal of Physics*, **50**, 753–758 (2000)

[6] Malashetty, M. S., Shivakumara, I. S., and Kulkarni, S. The onset of convection in a couple stress fluid saturated porous layer using a thermal non-equilibrium model. *Physics Letters A*, **373**, 781–790 (2009)

[7] Malashetty, M. S., Pal, D., and Kollur, P. Double diffusive convection in a Darcy porous medium saturated with couple stress fluid. *Fluid Dynamics Research*, **42**, 35502 (2010)

[8] Shivakumara, I. S. Onset of convection in a couple-stress fluid-saturated porous medium: effects of non-uniform temperature gradients. *Archive of Applied Mechanics*, **80**, 949–957 (2010)

[9] Malashetty, M. S. and Kollur, P. The onset of double diffusive convection in a couple stress fluid saturated anisotropic porous layer. *Transport in Porous Media*, **86**, 435–459 (2011)

[10] Srivastava, A. K., Bhadauria, B. S., and Mishra, P. Soret-driven double diffusive magneto-convection in couple stress liquid. *MATEC Web of Conference*, **1**, 06008-1-6 (2012)

[11] Kumar, A. V. and Gupta, V. K. Study of heat and mass transport in couple-stress liquid under g-jitter effect. *Ain Shams Engineering Journal*, **2016**, 1–12 (2016)

[12] Bhadauria, B. S., Siddheshwar, P. G., Singh, A. K., and Gupta, V. K. A local nonlinear stability analysis of modulated double diffusive stationary convection in a couple stress liquid. *Journal of Applied Fluid Mechanics*, **9**, 1255–1264 (2016)

[13] Kim, J., Kang, Y. T., and Choi, C. K. Soret and Dufour effects on convective instabilities in binary nanofluids for absorption application. *International Journal of Refrigeration*, **30**, 323–328 (2007)

[14] Siddheshwar, P. G., Kanchana, C., Kakimoto, Y., and Nakayama, A. Steady finite amplitude Rayleigh-Bénard convection in nanoliquids using a two-phase model-theoretical answer to the phenomenon of enhanced heat transfer. *ASME Journal of Heat Transfer*, **139**, 012402-1-8 (2016)

[15] Wang, S. and Tan, W. Stability analysis of Soret-driven double-diffusive convection of Maxwell fluid in a porous medium. *International Journal of Heat and Fluid Flow*, **32**, 88–94 (2011)

[16] Altawallbeh, A. A., Bhadauria, B. S., and Hashim, I. Linear and nonlinear double-diffusive convection in a saturated anisotropic porous layer with Soret effect and internal heat source. *International Journal of Heat and Mass Transfer*, **59**, 103–111 (2013)

[17] Gupta, U., Sharma, J., and Sharma, V. Instability of binary nanofluids with magnetic field. *Applied Mathematics and Mechanics* (*English Edition*), **36**(6), 693–706 (2015) DOI 10.1007/s10483-015-1941-6

[18] Agarwal, S. and Rana, P. Analysis of periodic and aperiodic convective stability of double diffusive nanofluid convection in rotating porous layer. *Applied Mathematics and Mechanics* (*English Edition*), **37**(2), 215–226 (2016) DOI 10.1007/s10483-016-2026-8

[19] Agarwal, S., Bhadauria, B. S., and Siddheshwar, P. G. Thermal instability of a nanofluid saturating a rotating anisotropic porous medium. *Special Topics and Reviews in Porous Media*, **2**, 1–12 (2011)

[20] Ren, Q. and Chan, C. L. Numerical study of double-diffusive convection in a vertical cavity with Soret and Dufour effects by lattice Boltzmann method on GPU. *International Journal of Heat and Mass Transfer*, **93**, 538–553 (2016)

[21] Hu, J., Benhadid, H., and Henry, D. Linear stability analysis of Poiseuille-Rayleigh-Bénard flows in binary fluids with Soret effect. *Physics of Fluids*, **19**, 034101 (2007)

[22] Ibrahim, F. S., Hady, F. M., Abdel-Gaied, S. M., and Eid, M. R. Influence of chemical reaction on heat and mass transfer of non-Newtonian fluid with yield stress by free convection from vertical surface in porous medium considering Soret effect. *Applied Mathematics and Mechanics* (*English Edition*), **31**(6), 675–684 (2010) DOI 10.1007/s10483-010-1302-9

[23] Nawaz, M., Hayat, T., and Alsaedi, A. Dufour and Soret effects on MHD flow of viscous fluid between radially stretching sheets in porous medium. *Applied Mathematics and Mechanics* (*English Edition*), **33**(11), 1403–1418 (2012) DOI 10.1007/s10483-012-1633-x

[24] Al-Odat, M. Q. and Al-Ghamdi, A. Numerical investigation of Dufour and Soret effects on unsteady MHD natural convection flow past vertical plate embedded in non-Darcy porous medium. *Applied Mathematics and Mechanics* (*English Edition*), **33**(2), 195–210 (2012) DOI 10.1007/s10483-012-1543-9

[25] Newell, A. C. and Whitehead, J. A. Finite bandwidth, finite amplitude convection. *Journal of Fluid Mechanics*, **38**, 279–303 (1969)

[26] Siddheshwar, P. G. and Titus, S. Nonlinear Rayleigh-Bénard convection with variable heat source. *ASME Journal of Heat Transfer*, **135**, 122502-1-12 (2013)

[27] Hu, J., Henry, D., Benhadid, H., and Yin, X. Transient growth in Poiseuille-Rayleigh-Bénard flows of binary fluids with Soret effect. *Applied Mathematics and Mechanics* (*English Edition*), **37**(9), 1203–1218 (2016) DOI 10.1007/s10483-016-2121-6

[28] Platten, J. K. and Chavepeyer, G. Finite amplitude instability in the two-component Bénard problem. *Proceedings of the Conference on Instability and Dissipative Structures in Hydrodynamics*, Advances in Chemical Physics (Eds. Prigogine, I. and Rice, S. A.), **32**, 281–322 (1973)